TM 5708 - 561 - 770
Sent: 6/13/97 2/345

AN ELECTROCHEMICAL APPROACH TO PREDICTING LONG-TERM LOCALIZED CORROSION OF CORROSION RESISTANT CONTAINER MATERIALS

Prepared for

Nuclear Regulatory Commission
Contract NRC-02-93-005

Prepared by

Darrell S. Dunn
Gustavo A. Cragnolino
Narasi Sridhar

Center for Nuclear Waste Regulatory Analyses
San Antonio, Texas

June 1997

3/3495

ABSTRACT

Lifetime predictions of containers used for the disposal of high-level radioactive waste (HLW) are necessary to determine the overall performance of a HLW repository. Failure of the containers by localized corrosion and release of radionuclides into the accessible environment may occur if chloride-containing groundwater infiltrates the repository. To assess the repository performance, it is necessary to develop a methodology for predicting the long-term susceptibility of container materials to localized corrosion. Laboratory tests have demonstrated that pitting and crevice corrosion are initiated when the corrosion potential of the material exceeds the repassivation potential for localized corrosion. Once initiated, the propagation rate for the localized attack will result in rapid penetration of the waste packages. However, no localized corrosion can be initiated and all active corrosion sites repassivate when the corrosion potential of the material is lower than the repassivation potential. The results of this investigation have identified the corrosion potential and the repassivation potential as useful parameters to predict the long-term localized corrosion susceptibility for corrosion resistant candidate container materials such as type 316L stainless steel and alloy 825.

CONTENTS

FIGURES

TABLES

ACKNOWLEDGMENTS

This report was prepared to document work performed by the Center for Nuclear Waste Regulatory Analyses (CNWRA) for the Nuclear Regulatory Commission (NRC) under Contract No. NRC-02-93-005. The activities reported here were performed on behalf of the NRC Office of Nuclear Material Safety and Safeguards (NMSS), Division of Waste Management (DWM). The report is an independent product of the CNWRA and does not necessarily reflect the views or regulatory position of the NRC.

QUALITY OF DATA, ANALYSES, AND CODE DEVELOPMENT

DATA: CNWRA-generated original data contained in this report meets quality assurance requirements described in the CNWRA Quality Assurance Manual. Sources for other data should be consulted for determining the level of quality for those data.

ANALYSES AND CODES: No computer code was used for analyses contained in this report.

1 INTRODUCTION

The U.S. Department of Energy (DOE) updated waste containment and isolation strategy (U.S. Department of Energy, 1996) for the proposed repository at the Yucca Mountain (YM) site has the primary goals of near-complete containment of radionuclides within waste packages (WP) for several thousand years and acceptably low annual doses to a member of the public living near the site. The WP consists of containers, fillers, basket materials, and waste forms [spent fuel (SF) or glass]. One of the most important system attributes recognized in this strategy is the container lifetime. In order to demonstrate container lifetime, the adequacy of methodologies for extrapolating short-term laboratory data to long-term performance in the repository should be evaluated.

Several WP designs have been evaluated by the DOE over the history of the YM repository program. Of these designs, the canistered fuel design is considered most likely to be used for high-level radioactive waste (HLW) disposal (TRW Environmental Safety Systems, Inc., 1996). In this design, either 21 pressurized water reactor (PWR) or 40 boiling water reactor (BWR) SF assemblies will be contained in a type 316L stainless steel (SS) multipurpose canister (MPC). The MPC (3.5 cm wall thickness) will be surrounded by an inner overpack made of a corrosion resistant alloy (2.0 cm wall thickness), which will in turn be contained in an outer overpack made of a corrosion allowance material (10 cm wall thickness). The total surface area of such a WP will be about 37 m^2 and the loaded weight about 65,000 kg. Alternate designs include WP for uncanistered fuel (no MPC), small canistered fuel (12 PWR or 24 BWR SF assemblies), and vitrified waste. Nickel base alloys such as alloys 825, 625, and C-22 are presently being evaluated for the inner corrosion resistant overpack and carbon steel, such as A 516 grade 55, is proposed for the outer corrosion allowance overpack (Roy et el., 1996). If the container should come in contact with groundwater, it is anticipated that the uniform corrosion of the carbon steel overpack will proceed at a slow and predictable rate. Evaporative effects and interactions with concrete in the repository may result in an alkaline groundwater that in the presence of chloride, can lead to localized corrosion of the carbon steel surface (Marsh et al., 1986). If the carbon steel overpack is perforated, then the inner overpack will exposed to the repository environment. Corrosion of the inner overpack may be mitigated by the use of both a corrosion resistant alloy and galvanic coupling of the inner overpack to the carbon steel overpack (Mohanty et al., 1996).

The traditional, and perhaps the most readily understood, approach to long-term corrosion prediction involves obtaining the corrosion rates of candidate materials exposed to environmental conditions that are similar to, or preferably more severe than, the anticipated environmental conditions of the particular application and integrating over time the corrosion rates to predict service life. The corrosion rates are obtained through the use of controlled laboratory tests, coupon exposures in the field, or performance of similar materials in analogous applications. An example of this approach may be found in the DOE Total System Performance Assessment (TSPA) conducted in 1995 (TRW Environmental Safety Systems, Inc., 1995), where atmospheric and natural-water corrosion data are used to estimate the corrosion rate of outer overpacks in the repository. For the corrosion resistant inner overpack, degradation is assumed to occur only by localized corrosion that is described by a pit growth rate that varies with temperature. The general corrosion rate for the inner overpack is not considered in the calculation of the container lifetime. This approach, referred to here as the empirical corrosion rate approach, has many drawbacks, when applied to corrosion estimates for the repository time scales (eg., 10^3–10^4 yr), as discussed in the following:

- The relationship between the laboratory or field service environments in which corrosion rates are obtained and the slowly evolving repository environment can seldom be clearly

established. This can be especially problematic in the case of the hydrologically unsaturated zone at the YM site, where the environment contacting the container (typically referred to as the near-field or very near-field environment) may vary in concentration from that of a dilute groundwater to that of a saturated electrolyte due to a complex combination of processes including evaporation, interaction with man-made materials, and radiolysis.

- Short-term corrosion rate data tend to be more useful in eliminating materials that are not applicable for a given environment than for predicting the long-term performance of materials. This is because many corrosion phenomena, especially localized corrosion and stress corrosion cracking (SCC), have relatively long initiation times that may be longer than the corrosion test period (Nakayama et al., 1993a). Once corrosion initiates, however, the rates can be quite high. The initiation time may itself be a function of the material and the test environment.

- It is difficult to evaluate the effects of design features such as galvanic coupling. Hence, a large number of long-term tests using various possible design features have to be conducted.

- Proof of the performance of a material in a repository cannot be obtained with the approach used in traditional engineering practice due to the lack of long-term exposure data. If feasible, models developed to simulate the long-term corrosion behavior of a material should be constructed from a mechanistic understanding of the uniform and localized corrosion processes. The predictive capability of the models can be verified using a diverse set of corrosion data. However, the empirical corrosion rate approach is not based on a mechanistic understanding of the processes involved. As a result, long-term estimation made using this approach are more uncertain. The usefulness of the empirical corrosion rate approach is further constrained when most of the field and laboratory measurements of corrosion rates do not include measurement of the corrosion potential of the metal in the test environment.

An electrochemical approach can overcome many of the limitations of the empirical corrosion rate approach either by explicitly calculating the corrosion rates in terms of constituent electrochemical reactions (Shoesmith et al., 1996; King and Kolar, 1996) or using critical electrochemical parameters for determining the onset of various corrosion processes (Sridhar et al., 1995; Mohanty et al., 1996). An electrochemical approach has several advantages:

- The occurrence of various corrosion modes such as pitting, crevice corrosion, and SCC can be accelerated in short-term tests using a range of environments and applied potentials. The critical potentials for the occurrence of various corrosion modes can then be identified. The extrapolation from these short-term data is then made by calculating the evolution of the natural potential of the metal (corrosion potential) in the repository environment and comparing these to calculations of the measured critical potentials. The corrosion and critical potentials can be supported by fundamental electrochemical models based on the kinetics of the corrosion reactions. Thus a clearer and more defensible relationship can be established between the test environments and the anticipated repository environment.

- The initiation time for localized corrosion and SCC can be explicitly considered in terms of its relationship to potential. The kinetics of the various corrosion modes can be measured independently and supported by electrochemical models.

- The corrosion performance of a given material in diverse applications can be assembled in a single map of critical electrochemical parameters, similar to the approach used by Staehle (1994), to provide greater confidence in the performance prediction. Electrochemical models do not dispense with the need to measure corrosion rates; rather, they assign different corrosion rates to different regimes of corrosion, with the delineation of the regimes of corrosion and the rates of corrosion within each regime supportable by fundamental, mechanistic reasoning. It must also be emphasized that electrochemical models, just as other models, are only as good as the quality of the underlying data. Here too, the electrochemical models offer an advantage over empirical corrosion rate models because they can be used to evaluate critical data needs.

A number of investigators have proposed the use of the repassivation potential, E_{rp}, as a parameter to predict the long-term initiation of localized corrosion (Dunn et al., 1996a; Dunn et al., 1995; Tsujikawa and Hisamatsu, 1984; Tsujikawa and Kojima, 1991) and SCC (Sridhar et al., 1995; Cragnolino et al., 1996). If the corrosion potential, E_{corr}, of the metal exceeds E_{rp}, then localized corrosion can be initiated. Prior to initiation of localized corrosion, the metal is expected to corrode at a slow rate corresponding to the passive current density of the metal and, after the initiation of localized corrosion, it would propagate through the metal container at a higher rate controlled by the diffusion of metal chloride species in the pit solution. If the E_{corr} of the inner barrier decreases below E_{rp}, localized corrosion would cease or repassivate. The concept of repassivation is not new. Pourbaix et al. (1963) proposed the use of the E_{rp} (also called the protection potential) below which localized corrosion would not be initiated. However, later investigations by Wilde (1974), and Rosenfeld et al. (1978) indicated that the E_{rp} decreased with increasing extent of prior corrosion, leading to the conclusion that this parameter cannot be used as a conservative criterion. Hence, to be a useful parameter for predicting long-term localized corrosion, it must be demonstrated that a lower bound value for E_{rp} can be established.

In this report, data generated by the Center for Nuclear Waste Regulatory Analyses (CNWRA) program on type 316L SS and alloy 825 during the past few years is reviewed along with data from the literature to demonstrate the conservatism of E_{rp}. Additionally, the applicability of E_{rp} for prediction of the long-term occurrence of localized corrosion is examined with the results of ongoing long-term tests. Finally, the mechanistic understanding of the localized corrosion initiation and repassivation processes is assessed.

2 EXPERIMENTAL METHODS

2.1 MATERIALS

A variety of corrosion resistant and corrosion allowance materials are being tested in this program (Sridhar et al., 1993b). However, this report focuses mainly on alloy 825 and type 316L SS because its objective is to establish the predictive methodology for corrosion resistant materials. The compositions of type 316L SS and alloy 825 are given in table 2-1.

Table 2-1. Composition of alloy 825 and type 316L stainless steel (weight percent)

Alloy	C	Cr	Cu	Fe	Mn	Mo	Ni	S	Ti
825	0.010	22.1	1.79	30.4	0.35	3.21	41.1	<0.001	0.82
316L	0.014	16.3	0.27	68.9	1.58	2.07	10.4	0.018	-

2.2 ENVIRONMENTS

Tests were conducted at 95 °C ±2 °C in an ASTM G-31 (American Society for Testing and Materials, 1996a) type electrochemical cell with approximately 1,500 mL of solution containing 1,000-ppm Cl^-, 85 ppm HCO_3^-, 20 ppm SO_4^{2-}, 10 ppm NO_3^-, and 2 ppm F^-, all as sodium salts. The effect of chloride concentration was studied by adding chloride as NaCl to the above solution. However, because of the solubility limitation, solutions with chloride concentration higher than about 5 molal were achieved by the use of LiCl or $MgCl_2$ solutions, without the addition of other anionic and cationic species. In tests conducted under air-saturated conditions, a high purity mixture of 79%N_2+ 21%O_2 (CO_2 free air or zero air) gas was used to purge the solution.

2.3 LOCALIZED CORROSION TESTS

The configurations of the various types of specimens used in pitting and crevice corrosion tests in this investigation are shown in figure 2-1 and discussed in the following:

- Cylindrical specimens of alloy 825 and type 316L SS measuring 6.2 mm in diameter and 48.6 mm long with a 600 grit finish (figure 2-1a) were used in cyclic, potentiodynamic polarization (CPP) tests. These tests were conducted in an ASTM G-5 (American Society for Testing and Materials, 1996b) type five-neck flask equipped with a calibrated thermometer, a platinum counter electrode, and a salt bridge with a porous silica tip filled with the test solution. The salt bridge was connected to a saturated calomel electrode (SCE) used as the reference electrode, that was maintained at room temperature. Test solutions were thoroughly deaerated with high-purity N_2 (99.999%) through a glass frit bubbler. Prior to the start of each test, the E_{corr} of the specimen was measured versus the reference electrode using a high-impedance (100M ohm) electrometer. Scans were started at the E_{corr} and reversed at a current density of 5 mA/cm^2, then stopped upon reaching the initial value of E_{corr}. A scan rate of 0.167 mV/sec was used in all CPP tests. Following each scan, the specimen was

examined for localized attack. The purpose of the CPP tests was to establish the initiation potentials for pitting (E_p) and crevice corrosion (E_{crev}), as well as E_{rp} over a wide range of environmental conditions (10^{-4} to 10 molal Cl^-, 25 to 95 °C).

- Simulated, single-pit propagation tests were conducted on alloy 825 using lead-in-pencil specimens as shown in figure 2-1b. The advantage of this geometry is that the location of pitting is known and it is amenable to theoretical analyses using relatively simple analytical models. The disadvantage of the single-pit specimen is that the morphologies and growth rates of naturally formed pits cannot be studied. Prior to the start of the tests, the specimens were weighed to ±0.03 mg. The specimens were then covered with a polyolefin tubing that allowed only one end of the specimen to be exposed to the solution. Electrical contact to the specimen was made outside the test cell. The specimen was oriented so that the opening of the unidirectional pit faced upwards. The pit had an area of 0.041 cm^2. Corrosion was initiated at potentials of 500 to 600 mV_{SCE}. After sufficient growth, the potential was decreased to values in the range of −300 to 100 mV_{SCE} at a rate of 5 mV/sec. The current and potential were recorded allowing real time calculation of pit depth and propagation rate. This calculation was made using the theoretical weight loss of 2.64×10^{-4} g/coulomb assuming congruent dissolution of Fe, Cr, and Ni in alloy 825 as Fe^{2+}, Cr^{3+} and Ni^{2+}, respectively (Dunn et al., 1993). At the conclusion of the tests, the specimens were reweighed to confirm the accuracy of the propagation rate calculations. The purpose of these tests was to measure the growth rate and repassivation of single pits and compare them to measurements made on samples where an uncontrollable number of multiple pits formed.

- Potentiostatic polarization tests were conducted using cubic specimens, shown in figure 2-1c, having a total surface area of 15 cm^2, that includes both polished and chromium-depleted mill-finished surfaces, as described in previous publications (Dunn et al., 1993; Dunn et al., 1995). Potentiostatic and open-circuit corrosion tests were also conducted using specimens with a controlled crevice (figure 2-1d). Potentiostatic pitting and crevice corrosion initiation times were measured by polarizing both cylindrical and creviced specimens to potentials above and below the E_{rp} measured in CPP tests. Specimens were connected to a computer-controlled multichannel potentiostat. A constant potential was applied for test intervals of 28 days. Between these test periods, the specimens were examined for weight loss (± 0.00015 g) and visible signs of corrosion while the test solution was changed. No further exposures were conducted on specimens after localized corrosion occurred. Open-circuit tests were conducted with a setup and solutions similar to those used for the potentiostatic polarization tests. However, instead of controlling the specimen with a potentiostat, the corrosion potential of alloy 825 was continuously monitored in air-saturated, 1,000-ppm chloride solutions at 95 °C. Periodically, the test was interrupted and the specimen was examined for signs of localized corrosion. These methods allowed the validity of using E_{rp} from short-term CPP tests as a parameter for determining long-term performance to be tested.

- At open circuit, no net current flows in the system. As a result, the corrosion kinetics cannot be measured using electrochemical techniques on a single specimen. Hence, another series of open-circuit corrosion tests was conducted with a creviced alloy 825 specimen connected to a large noncreviced alloy 825 plate through a zero resistance ammeter (ZRA). If crevice

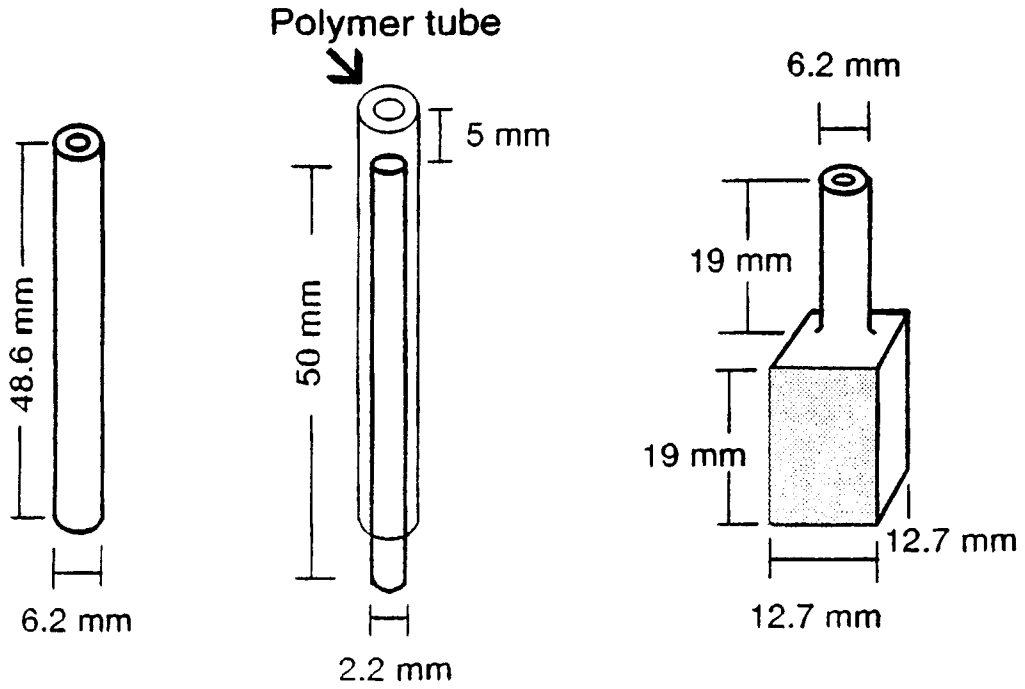

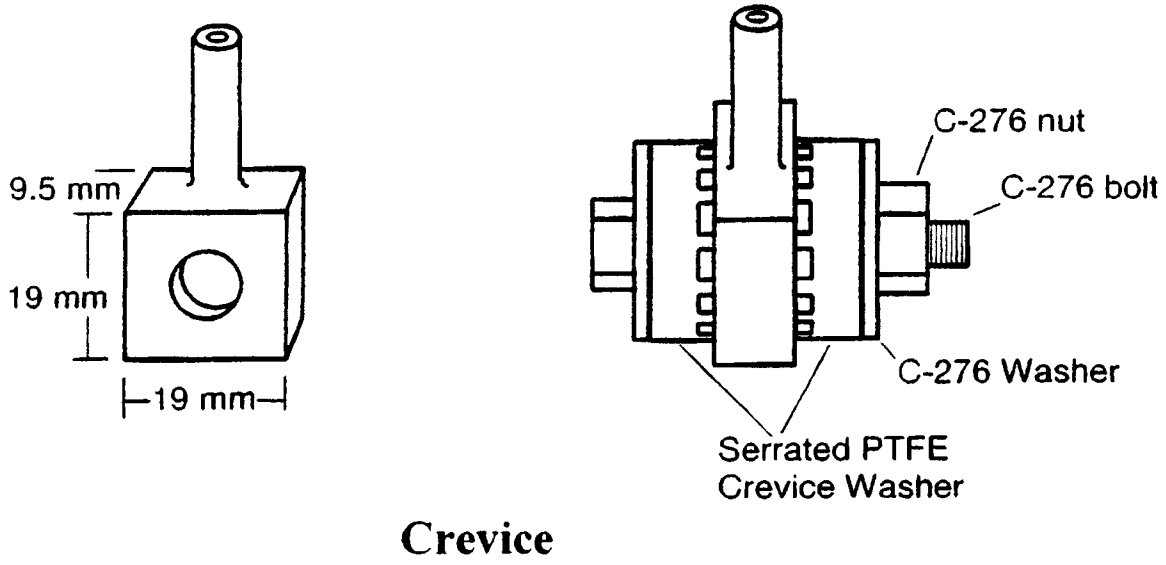

Figure 2-1. Schematic illustration of various specimen configurations used in the study of localized corrosion

corrosion occurred, the potential of the crevice specimen would decrease, resulting in a restoring current in the external circuit. The tests were conducted in solutions containing only 1,000 ppm chloride at 95 °C ±2 °C. The redox potential of the test solution was controlled by using a redox couple such as Cu^{+}/Cu^{2+} added as chloride salts with HCl or NaCl additions to achieve the desired total chloride concentration. The noncreviced to creviced specimen area ratio for all these tests was at least 10:1. During the tests, the current was measured with a resolution of 1 nA. The potential of the specimens was also recorded with a resolution of 0.1 mV with a SCE reference electrode maintained at room temperature. This test method allowed the measurement corrosion rate under natural exposure conditions at various redox potentials.

- Pit repassivation tests were also conducted on alloy 825 specimens shown in figure 2-1a. The tests were conducted by initiating pits at 600 mV_{SCE}. After initiation, the pits were grown at 400 mV_{SCE}. Following the accumulation of a specified charge density, the applied potential of the specimens was decreased to the desired value. The repassivation time was measured as the time required for the current density to decrease below 50 $\mu A/cm^2$ after the potential of the specimen was decreased rapidly from 400 mV_{SCE} to the desired potential. Details of this technique have been previously published (Sridhar et al., 1995; Dunn et al., 1996a). These tests allowed the validity of E_{rp} to be tested on specimens with multiple pits.

3 RESULTS

The effects of chloride concentration on E_p and E_{rp} of type 316L SS and alloy 825, as measured in CPP tests, are shown in figures 3-1 and 3-2, respectively. It is apparent that both E_p and E_{rp} are strongly dependent on the concentration of chloride. At chloride concentrations less than 10^{-3} M, the E_p and the E_{rp} are almost identical. It must be noted that the 95 percent confidence intervals on the repassivation potential for alloy 825 (figure 3-2) are rather large at chloride concentrations less than 10^{-2} M. This reflects the fact that pitting did not occur in all the specimens tested in low chloride concentration solutions. Where pitting did not occur, the E_{rp} has no physical meaning, the high value essentially reflecting the hysteresis in the oxygen evolution kinetics on the alloy. This results in a large scatter in the data. At chloride concentrations in the range of 10^{-2} to 1 M, a large difference between E_p and E_{rp} is observed. The critical potentials for alloy 825 are higher than those for type 316L SS, especially at low chloride concentrations. However, the difference between these potentials is significantly reduced at very high chloride concentrations. Another notable observation (figure 3-2) is the relative independence of E_{rp} with pH over a wide range, which is consistent with the observations in the literature and current understanding of pitting process. The independence of E_{rp} from external pH stems from the fact that the pH inside the pit is dictated by the hydrolysis of cations and becomes independent of the external pH. Regression lines through the E_p and E_{rp} data at chloride concentrations above 10^{-3} M were used to obtain expressions for these parameters in terms of Cl^- concentration and temperature. For alloy 825, one regression line is used for Cl^- concentrations from 10^{-3} to 3 M. A second regression line is used for Cl^- concentrations above 3 M. The general expression for E_{rp} is given in Eq. (3-1), with specific parameters for alloy 825 over the Cl^- concentration range of 10^{-3} to 3 M in Eq. (3-2):

$$E_{rp} = E^0_{rp}(T) + B(T)\,\mathrm{Log}\,[Cl^-] \tag{3-1}$$

$$E^0_{rp}(T) = 181.8 - 4.1\,(T); \quad B\,(T) = -305.0 - 0.8\,(T) \tag{3-2}$$

where, E_{rp} in mV_{SCE} is the repassivation potential for localized corrosion (pitting and crevice corrosion), and $E^0_{rp}(T)$ in mV_{SCE} is the repassivation potential at 1 M chloride concentration Eq. (3-1).

Previous work has established the dependence of E_{rp} on other environmental factors such as the concentrations of NO_3^-, SO_4^{2-} and F^- (Cragnolino and Sridhar, 1991). As shown in figures 3-1 and 3-2, thiosulfate ($S_2O_3^{2-}$) decreases the E_{rp} significantly for both alloys. The effect of $S_2O_3^{2-}$ observed in this study is similar to that found by Nakayama et al. (1993b). The corrosion potential data measured under various redox conditions (air, H_2O_2) of the solutions are also plotted in figures 3-1 and 3-2. As mentioned before, the occurrence of localized corrosion in a given environment can be gauged by comparing the E_{corr} under anticipated redox conditions and E_{rp} in the same environment, but without the redox species. While redox species such as oxygen and hydrogen peroxide are not expected to alter the E_{rp} significantly, it is generally convenient to obtain E_{rp} values in the absence of these redox species in order to expand the range of potentials studied. From figures 3-1 and 3-2, it may be anticipated that type 316L SS will suffer from localized corrosion in air-saturated chloride solution at chloride concentrations greater than

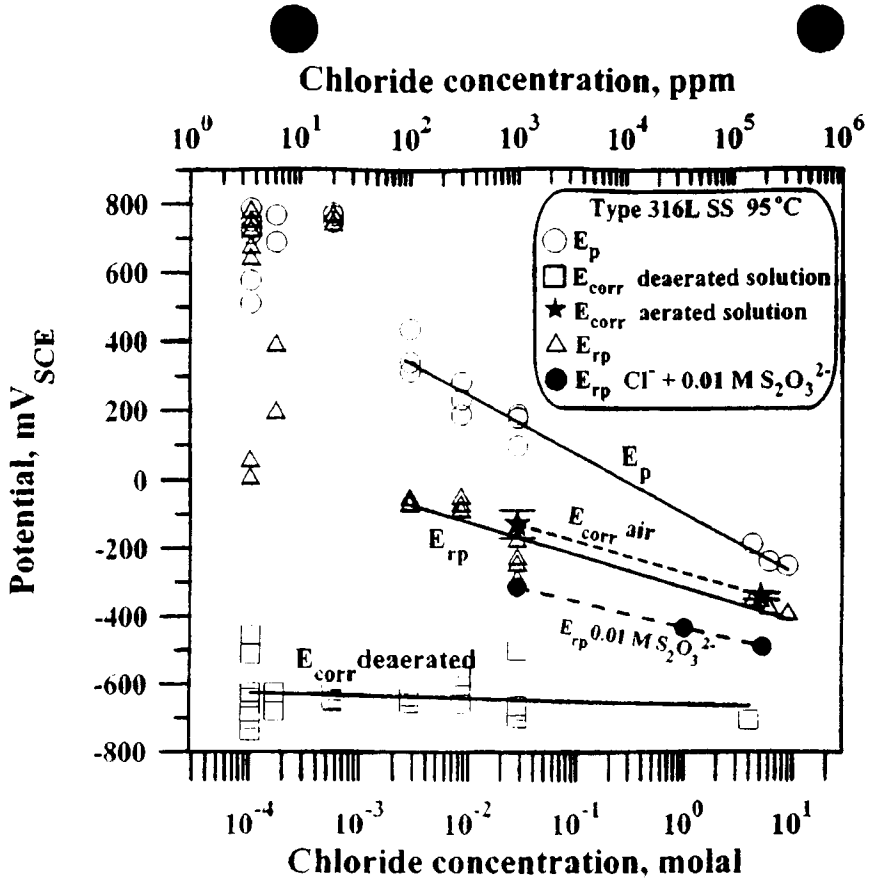

Figure 3-1. The effect of chloride concentration on critical potentials for pitting of type 316L stainless steel. Note that the specimens were completely immersed exposing the crevice between the specimen and washer. The scan rate was 0.167 mV/sec. All environments were deaerated.

10^{-3} M, whereas alloy 825 will not suffer localized corrosion in air-saturated solutions even at chloride concentrations as high as 4 M. However, the E_{corr} shown in these figures were obtained after only 1 hr of immersion. In the long term, the E_{corr} increases with time. This is indicated for alloy 825 in a 1,000-ppm solution in figure 3-3. Despite the erratic nature, a trend of an increasing E_{corr} is readily apparent. Over the course of almost 600 days of testing, the E_{corr} increased from an initial value of -270 mV_{SCE} to a high of 160 mV_{SCE}. The E_{rp} values ranging from 0 to 100 mV_{SCE} for this environment are also indicated in this figure. This range of E_{rp} values for alloy 825 in 1,000-ppm Cl^- has been reported previously (Dunn et al., 1996b). After approximately 350 days, the E_{corr} exceeded the E_{rp} and crevice corrosion was observed visually. Although depth of attack in each case was shallow and the weight loss minimal, crevice corrosion was visually observed each time E_{corr} exceeded E_{rp}.

The effect of pit depth on the E_{rp} for pitting and crevice corrosion is shown in figure 3-4. These tests were conducted by initiating pitting or crevice corrosion at potentials of 500 to 600 mV_{SCE}. After initiation, the localized corrosion was allowed to propagate at 400 mV_{SCE} (Sridhar et al., 1993a). The specimens were then repassivated by reducing the potential at a rate of 5 mV/sec until the current density was continuously below 50 $\mu A/cm^2$. After repassivation, the depth of the pits in open specimens and in crevice corroded regions was measured. The E_{rp} values obtained are plotted versus the depth of attack measured after the conclusion of the tests. By varying the time in which the localized attack was allowed

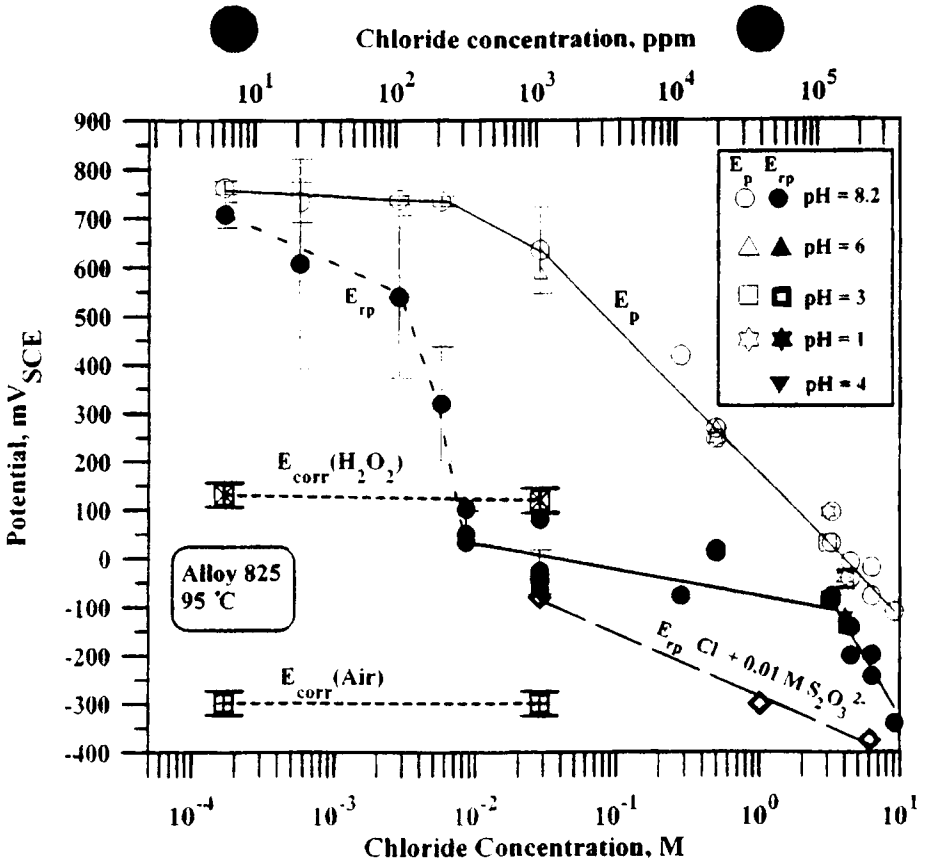

Figure 3-2. The effect of chloride concentration on critical potentials for pitting of alloy 825. Note that the specimens were completely immersed exposing the crevice between the specimen and washer. The scan rate was 0.167 mV/sec. All environments were deaerated.

to propagate, the relationship between depth of attack and E_{rp} can be determined. From the results plotted in figure 3-4, there is a strong dependence of pit and crevice corrosion depth on E_{rp} for shallow penetrations. However, when the depth of attack is deep, the E_{rp} appears to approach a lower limit. This is especially evident for the crevice corrosion data where the attack was allowed to propagate to depths greater than 1.0 mm. For shallow penetrations, there is considerable scatter in the crevice corrosion E_{rp} data. This can be related to the location of the localized attack within the crevice region. The total electrolyte pathway includes the pit depth and the depth into the crevice. Due to the stochastic nature of pitting, pits did not always occur at the same location inside the crevice. If the depth at which pits occurred inside the crevice is added to the depth of pits in the crevice, then the curve for crevice corrosion would move to the right.

The effect of applied potential as well as corrosion potentials under various redox conditions on the time to initiate localized corrosion is shown in figure 3-5. At potentials near the E_p measured in CPP tests (e.g., 600 mV_{SCE},) the initiation time was on the order of 200 sec. Decreasing the potential to 500 mV_{SCE} resulted in initiation times of 200,000 sec. In contrast, relatively short initiation times for crevice corrosion were observed even at applied potentials several hundred millivolts below the E_p. Figure 3-5 also shows pitting and crevice corrosion initiation time for specimens at open-circuit potentials under various redox conditions (1,000-ppm Cl^- solutions with Cu^{2+}/Cu^+ redox couple). The error bands in these data points denote the variation in the corrosion potentials for the same redox couple used. No pitting corrosion was observed on the boldly surfaces of any of the creviced specimens. In addition, no pitting corrosion was

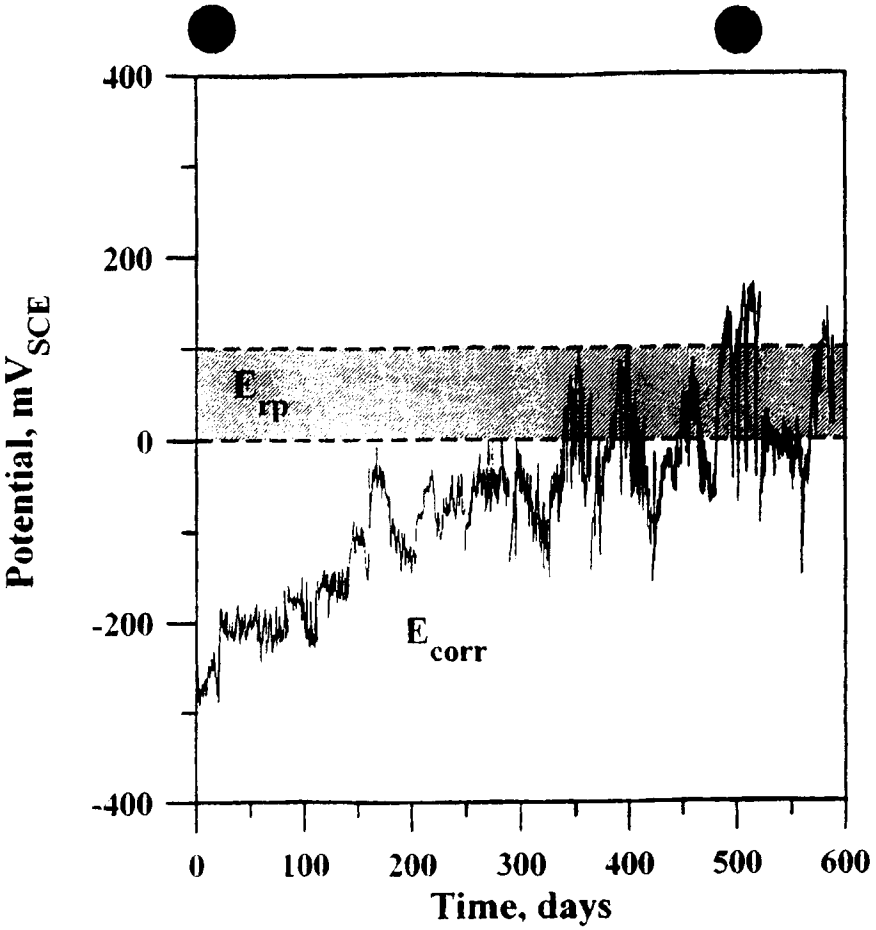

Figure 3-3. The evolution of corrosion potential of alloy 825 exposed to a 1,000-ppm chloride solution at 95 °C. Crevice corrosion was observed when E_{corr} exceeded the E_{rp} measured in short-term tests.

observed on a boldly exposed specimen in which the open-circuit potential was in the range of 300 to 440 mV_{SCE}. It is clear that the initiation time for pitting and crevice corrosion under natural exposure conditions is consistent with that under applied potential conditions. For clarity, the data for repassivation time are not shown in this figure. However, as discussed in a previous publication (Dunn et al., 1996a), the repassivation time increases with an increase in potential. The E_{rp} for alloy 825 is also shown in figure 3-5. It is evident that the initiation time for localized corrosion increases as the potential is decreased and approaches E_{rp}. Long-term tests are ongoing at various applied and natural potentials on alloy 825. One such test is shown in figure 3-6 for a specimen tested in 1,000-ppm chloride solution at an applied potential of 0 V_{SCE}, which is 100 mV below the critical potential. The test data for 1,000 days shows that initially the specimen had a current density of 8×10^{-5} A/cm^2 as well as some current spikes associated with the dissolution of the Cr^- depleted surface layer. In the later stages of the test, the current density was much lower, on the order of 1.0×10^{-7} A/cm^2. In addition, the weight of the specimen remained relatively constant and no localized corrosion has been observed.

Figure 3-7 shows current density versus time for creviced alloy 825 specimens maintained at potentials between 300 mV_{SCE} and 500 mV_{SCE}. At the higher potentials, the current density quickly increased, indicating that crevice corrosion had been initiated. In contrast, at lower potentials, significant increases in the current density are observed only after some incubation time. At the conclusion of the tests, all

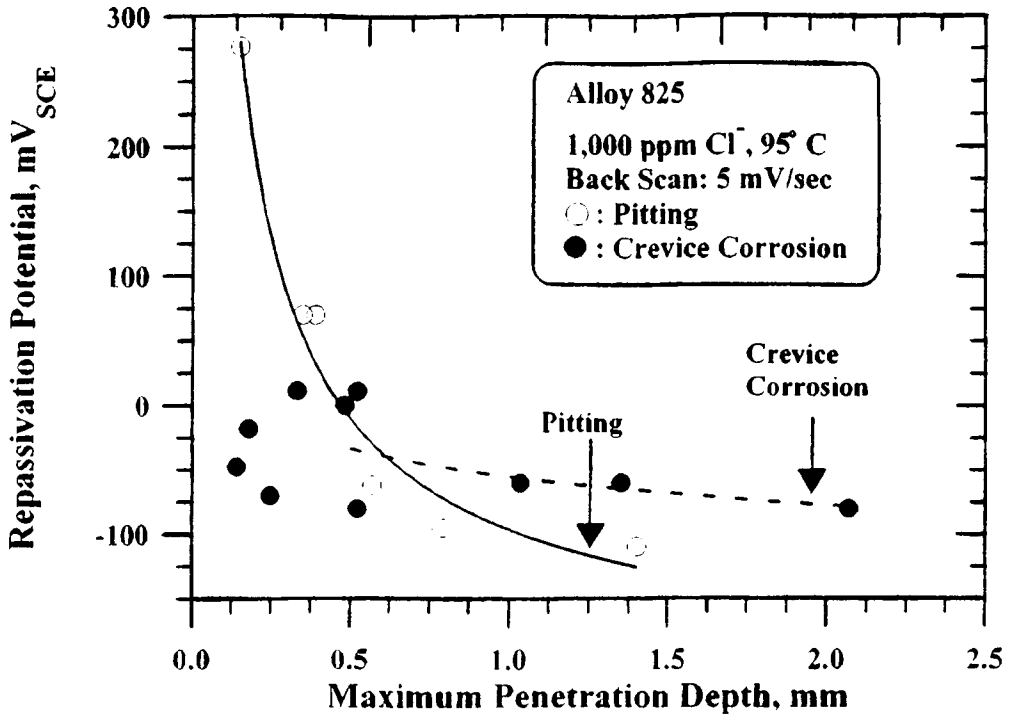

Figure 3-4. The effect of prior pitting and crevice corrosion depth on E_{rp} for pitting and crevice corrosion for alloy 825 in 1,000-ppm chloride solution at 95 °C

specimens were examined. For the specimens tested at 400 mV_{SCE} and above, crevice corrosion was initiated on at least 14 of 24 crevices formed by the serrated polytetrafluoroethylene (PTFE) crevice washer. For the specimens tested at potentials of 350 mV_{SCE} or less, only three or four crevices actively corroded. It should be noted that, for all specimens, the current density was calculated using only the area of the corroded regions. Each individual crevice had a surface area of 0.06 cm^2 yielding a total creviced area of 1.44 cm^2 using two serrated crevice washers with 12 teeth per washer.

To better understand the pit growth and repassivation process, pit propagation tests were conducted on alloy 825 using simulated, unidimensional, single-pit specimens with initial pit depths of 5 mm in a 1,000-ppm chloride solution at 95 °C. The pits were activated at 500 to 600 mV_{SCE} before the potential was decreased to values in the range of −300 to 100 mV_{SCE}. The results for several tests conducted with an initial pit depth of 5 mm are shown in figure 3-8. When the potential is decreased from 600 mV_{SCE} to −300 mV_{SCE}, the current density rapidly decreases and then returns to values in the range of 10^{-4} A/cm^2. After several hours at this value, the current slowly decreases to values less that 10^{-7} A/cm^2 before becoming negative. After repassivation of the pit, the calculated propagation rate is less than 10^{-10} cm/sec. As in the case of boldly exposed specimens, the time required for repassivation increased with an increase in potential. While some crevice corrosion occurred on all test specimens, the degree of crevice corrosion was found to be much greater at 0 mV_{SCE}. However, with time, complete repassivation of the pits was observed at potentials less than E_{rp}.

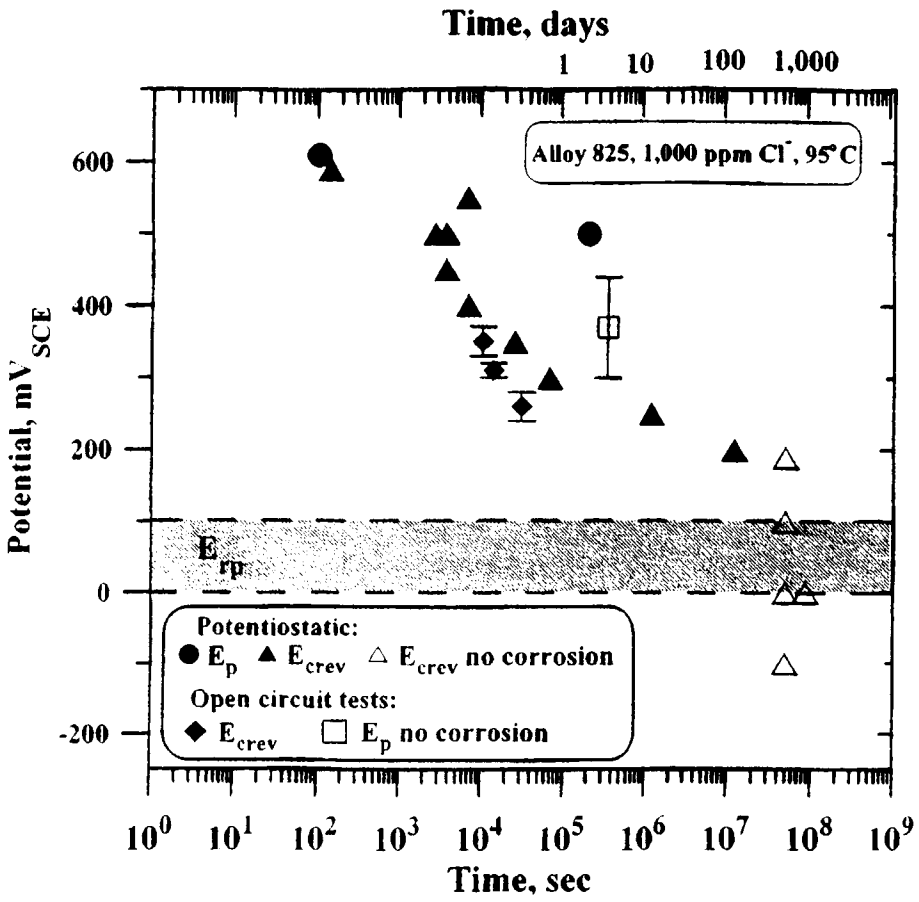

Figure 3-5. The effect of applied and corrosion potentials under various redox conditions on pitting and crevice corrosion initiation time for alloy 825 in 1,000-ppm chloride solution at 95 °C

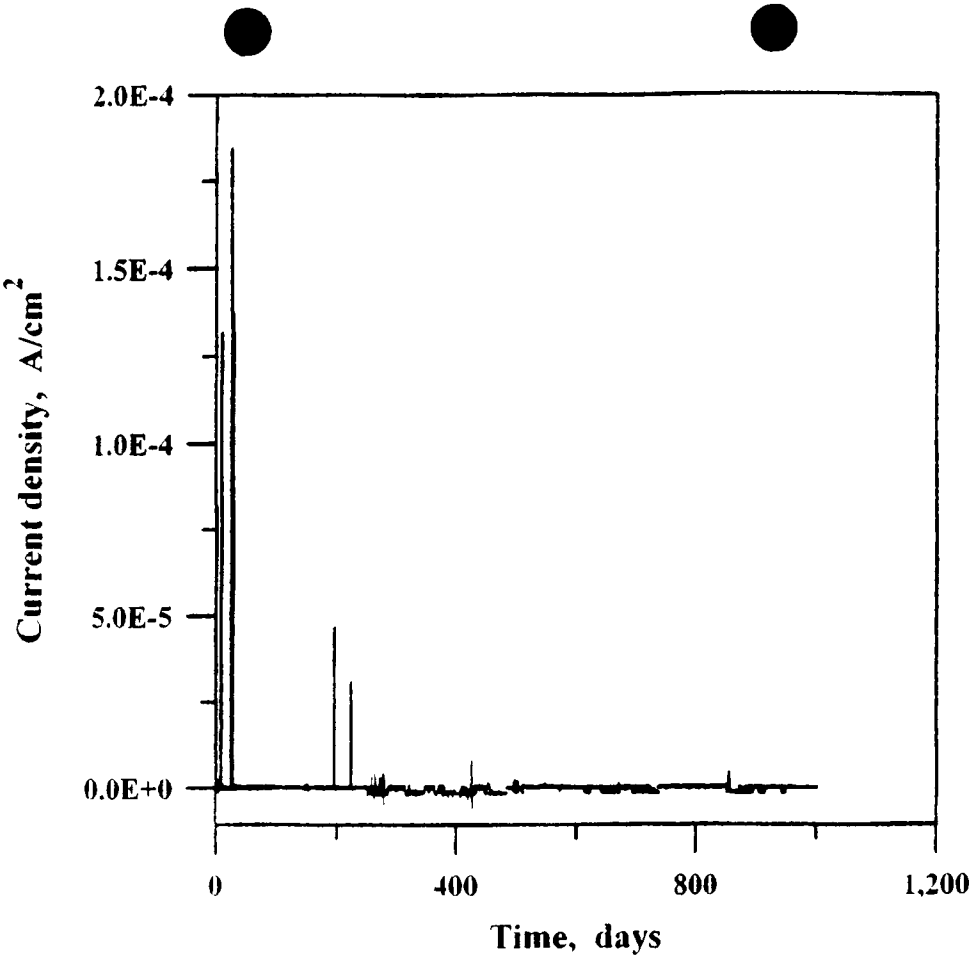

Figure 3-6. The current density for alloy 825 in 1,000-ppm chloride solution at 95 °C held at 0 mV_{SCE}, which is 100 mV below the E_{rp}

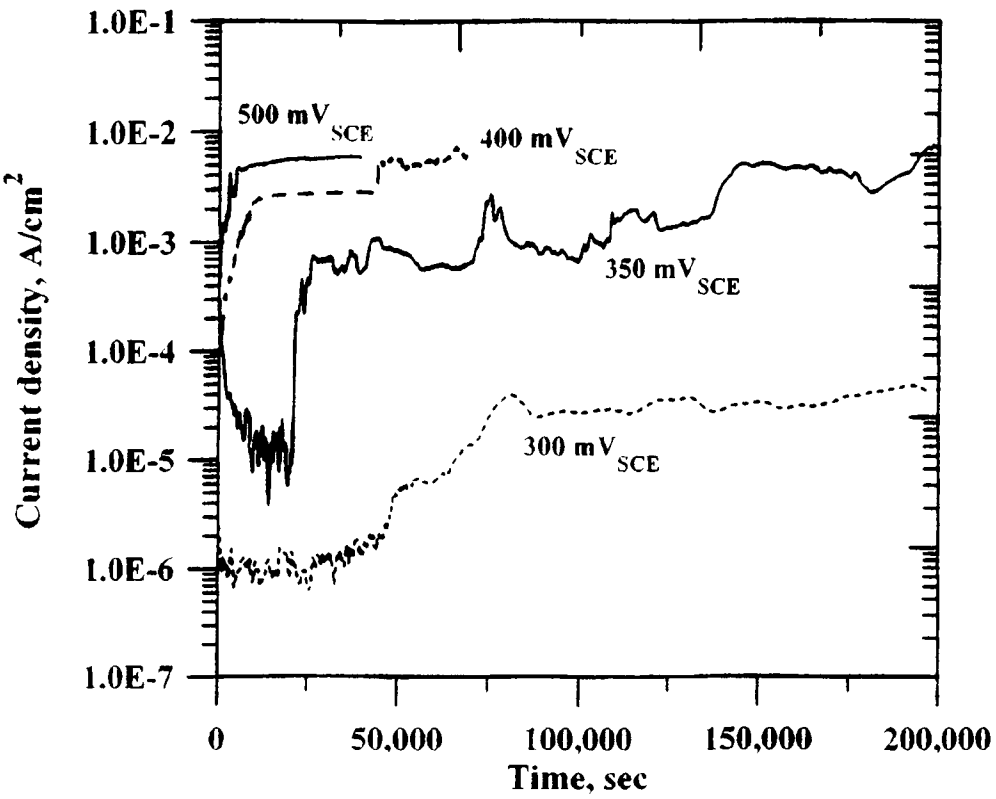

Figure 3-7. The effect of applied potential on crevice corrosion growth under multiple crevice washer. Alloy 825 in 1,000-ppm chloride solution at 95 °C.

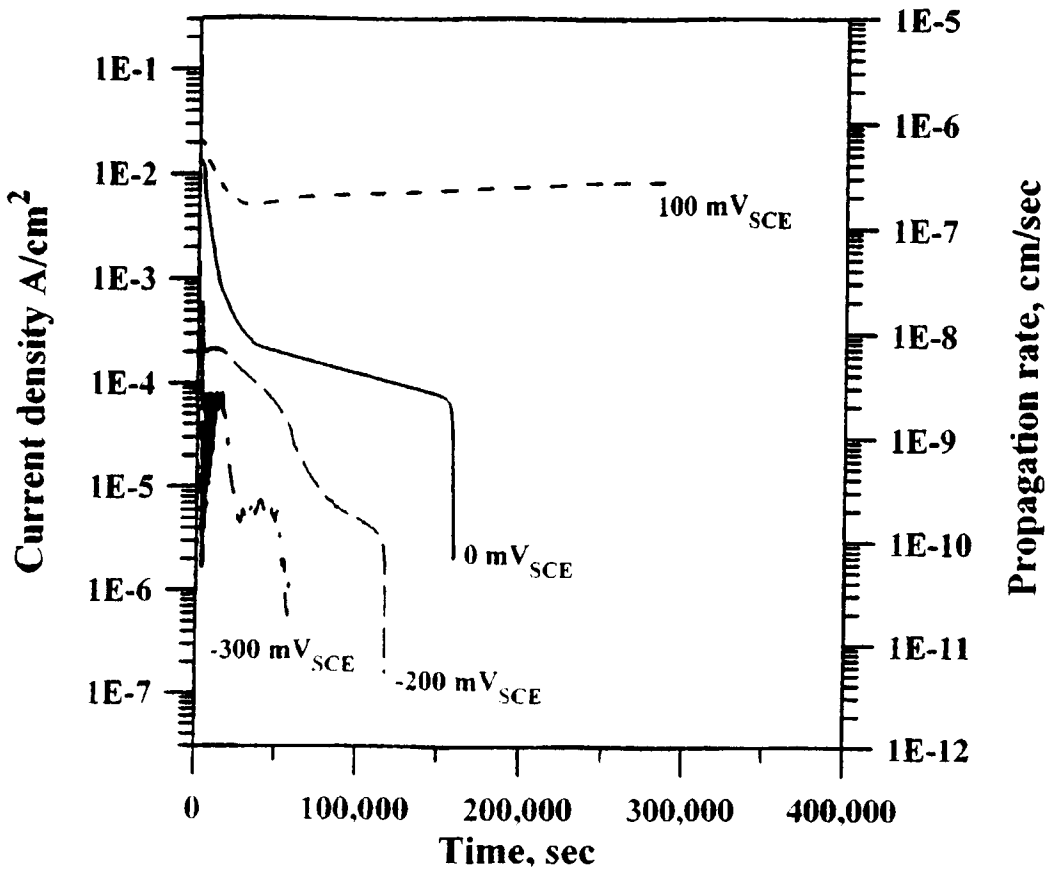

Figure 3-8. The effect of applied potential on single-pit growth rate using a lead-in-pencil type electrode. Alloy 825 in 1,000-ppm chloride solution at 95 °C.

4 DISCUSSION

4.1 SIGNIFICANCE OF REPASSIVATION POTENTIAL

The results shown in this report have been used in the Engineered Barrier System Performance Assessment Code (EBSPAC) to predict HLW container lifetimes (Mohanty et al., 1996). As discussed in the introductory section, the E_{rp} is used as a threshold parameter and the E_{corr} is used as an enabling parameter that triggers localized corrosion and SCC when it exceeds E_{rp}. For deep pits and crevices, E_{rp} is dependent on only the material, Cl^- concentration of the bulk environment, and temperature. Hence, for a given material/environment combination, the E_{rp} is a stable parameter that is independent of time. In the specific case of a HLW repository, the environment surrounding the waste packages will vary with time. Modeling calculations have predicted that the oxygen concentration, pH, temperature, and Cl^- concentration will change significantly after emplacement of the HLW (Sagar, 1997). As shown in figures 3-1 and 3-2, E_{rp} can be measured rather rapidly using the CPP technique and can be expressed in terms of a well established logarithmic relationship to the Cl^- concentration (Szklarska-Smialowska, 1986). The reduction in E_{rp} as the Cl^- concentration and temperature are increased indicates that, in environments with low Cl^- concentrations (and/or low temperatures), a high E_{corr} is needed to initiate localized corrosion. However, as the aggressiveness of the environment is increased, localized corrosion can be initiated at lower values of E_{corr}. One of the important findings of this study is the constancy of E_{rp} with depth of pitting or crevice corrosion beyond a certain depth. As mentioned previously, the use of E_{rp} fell into disfavor because some investigators showed that there was no lower bound value for E_{rp}. The effect of pit depth (in terms of charge density) on E_{rp} for a variety of alloy-environment combinations, as compiled from the literature data, is shown in figure 4-1. The absolute value of E_{rp}, of course, varies between systems, but it is clear that, if sufficient pit growth occurs, the E_{rp} attains a stable, lower-bound value. For shallow pit depths, it can be seen that the E_{rp} is a strong function of depth for all of the systems investigated. At a more microscopic scale, experiments on thin films have shown that E_{rp} initially decreases with pit growth, but then increases slightly and attains a stable value (Frankel et al., 1996). From this figure, it can also be seen that the early conclusion of Wilde (1974) that E_{rp} is not a bounding parameter was based on experiments where pit growth was insufficient.

Studies conducted at the CNWRA (Sridhar and Cragnolino, 1993) and elsewhere (Sugimoto and Asano, 1990) have shown that, while E_{rp} is a lower bound value independent of pit depth, it is dependent on test technique, specifically the backward scan rate from pit growth potential. The repassivation potential is known to be a function of scan rate (Szklarska-Smialowska, 1986), but thus far in the literature the scan rate effect has confounded two factors: the effect of forward scan rate on the extent of pit growth and the effect of backward scan rate on time needed for repassivation. Dunn et al. (1996a) have shown that the time required to repassivate a pit of given depth at any potential increased with the potential. Thus, a slower backward scan rate would be expected to result in higher E_{rp}. This accounts for slightly lower E_{rp} values presented in figure 3-3 (backward scan rate of about 0.5 mV/sec) compared to those plotted in figure 3-2 (scan rate of 0.167 mV/sec) for a chloride concentration of 1,000 ppm (0.028 molal). The E_{rp} measured using the lead-in-pencil type electrode (figure 3-8) was higher than that of the CPP tests despite a much deeper pit (5 mm). These experiments had the slowest scan rate because they were conducted

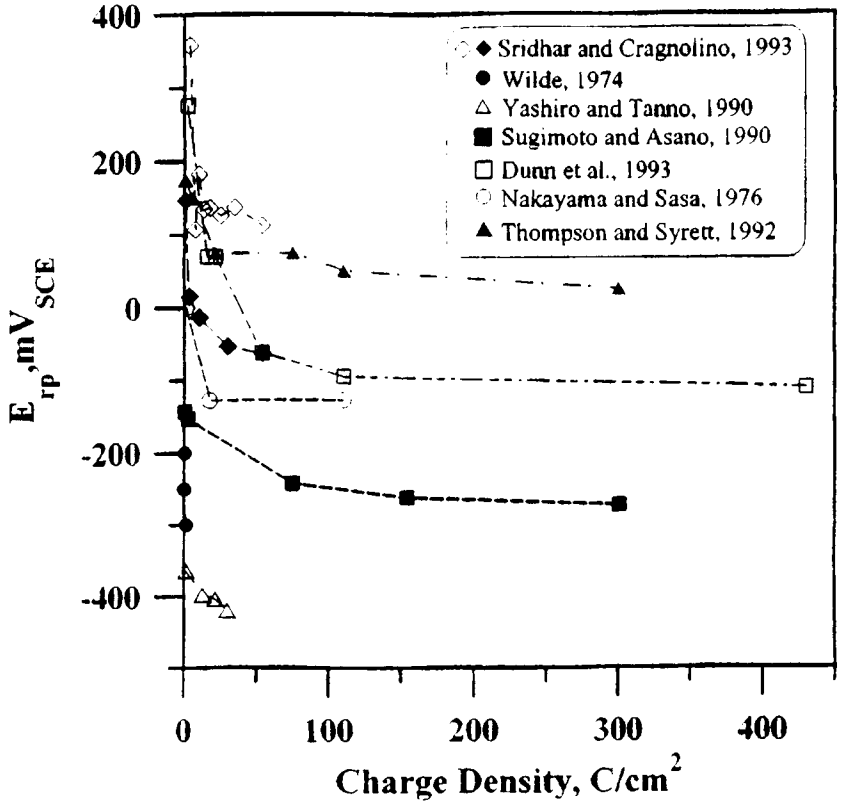

Figure 4-1. The effect of pit/crevice depth on E_{rp} on a number of alloy-environment combinations as found by a variety of investigators

potentiostatically. From the perspective of long-term prediction, since the potential is expected to change slowly over time, the lower predicted E_{rp} from short-term tests is conservative.

Potentiostatic testing carried out for times ranging from a few days to over 1,000 days clearly indicates that localized corrosion can be initiated at potentials far less than the E_p measured in CPP tests (figure 3-5). Thus, the E_p measured in CPP tests is not a useful parameter to predict the long-term initiation of localized corrosion. At potentials close to E_p, multiple sites of crevice corrosion were observed to be initiated. As the potential was reduced, the number of active sites decreased. For specimens tested at potentials near the E_{rp}, localized attack usually only occurred at one site. From the results shown in figure 3-5, it is apparent that the initiation time for the creviced specimens under applied potentiostatic control compared well with the initiation times measured in open-circuit tests with Cu^{2+}/Cu^{+} redox couple added to the solutions to increase the redox potential of the environment. These data provide increased confidence that the concept of repassivation potential can be applied to materials exposed to natural redox

conditions. No localized corrosion has been initiated to date at potentials below the E_{rp} even after 1,000 days of testing.

4.2 PIT PROPAGATION RATE

Results obtained with alloy 825 single-pit specimens indicate that, at potentials below the E_{rp}, the propagation rate for pitting corrosion is approximately the same as the passive dissolution of alloy 825. At potentials above the E_{rp}, the pits propagated at a very rapid rate. However, it is important to note that these pit growth rates are obtained under potentiostatic conditions where there is no cathodic limitation. Additionally, the geometry of the single-pit specimens used inert walls that did not allow the lateral propagation of the localized corrosion front. Thus, the cylindrical pits formed using these specimens do not represent pitting under natural conditions. The measured crevice corrosion propagation rate for type 316L SS in 1 M chloride solution is shown in figure 4-2. These measurements of the propagation rates of pits in creviced specimens from open-circuit tests (Dunn et al., 1996b) indicate that the propagation rates at open-circuit, while still unacceptably high, decrease with time. The rate-controlling process for crevice corrosion growth under natural potential conditions is not clear at this time. The exponent of −0.62 in the rate equation lies between −0.5 for transport or internal ohmic controlled pit growth and −0.67 for external ohmic controlled pit growth mechanisms. In either case, these results clearly indicate that the pitting multiplication factor approach used in some performance assessment models, such as that in DOEs TSPA (TRW Environmental Systems, Inc., 1995), is not valid for corrosion resistant materials.

4.3 LONG-TERM PREDICTION OF LOCALIZED CORROSION

In order for localized corrosion to be initiated in a repository setting, the E_{corr} of the corrosion resistant barriers must be greater than the E_{rp}. Initial measurements of the E_{corr} for type 316L SS shown in figure 3-1 indicate that localized corrosion in deaerated environments is not likely. However, the E_{corr} is greater than E_{rp} in air-saturated environments and the possibility of localized corrosion exists. Although clearly more resistant, especially at low chloride concentrations, alloy 825 is also susceptible to localized corrosion when the E_{corr} of the specimen exceeds E_{rp}. Long-term corrosion potential data for alloy 825 in a 1,000-ppm Cl^- based solution are shown in figure 3-3. The increase in the corrosion potential of this specimen is most likely the result of several factors:

(i) The mill finished surface, which has previously been shown to be deficient in Cr compared to the bulk material, corrodes at a faster rate than the polished surfaces. This is supported by the initial weight loss observed in the early stages of exposure. The Cr-depleted layer yields a lower E_{corr} because it is more active.

(ii) After the Cr-depleted layer has been removed, the exposed surface contains an increased amount of Cr. The passive film formed has improved corrosion resistance and the passive current density decreases.

As a result the corrosion potential increases since it is determined by the point where the sum of all anodic currents and all cathodic currents equals zero. A similar increase in E_{corr} is observed with thermally oxidized specimens. The corrosion potential of alloy 825 in air-saturated 1,000-ppm chloride solutions increased by as much as 200 mV after dry thermal oxidation at 100 °C for 30 days (Dunn et al.,

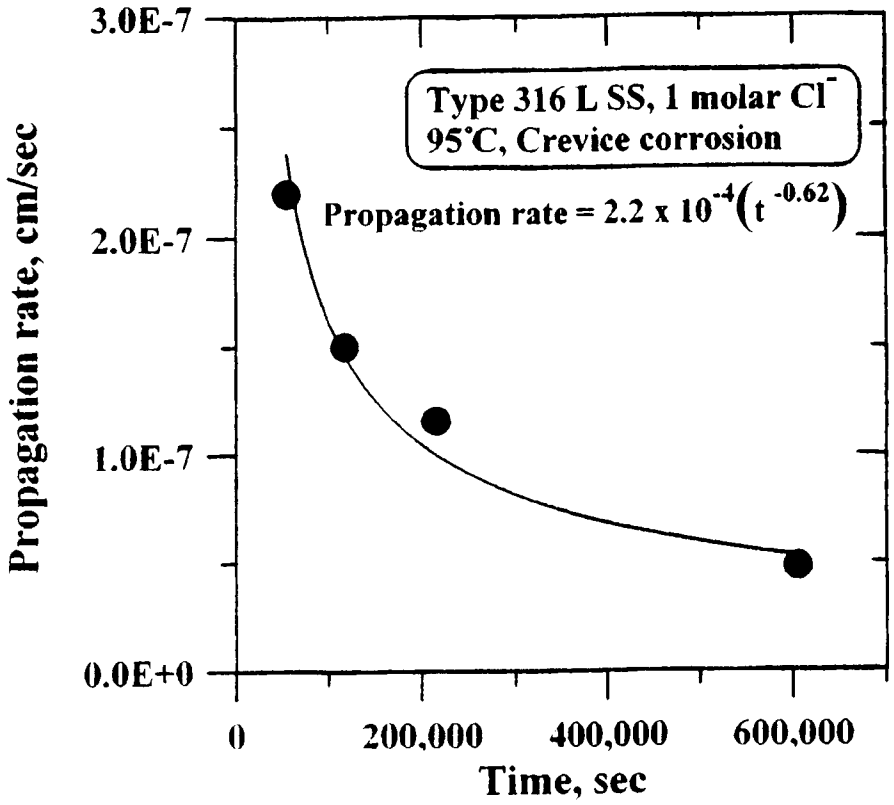

Figure 4-2. Crevice corrosion growth rate of type 316L stainless steel under open-circuit conditions in a 1 M chloride solution

1993) prior to exposure to aqueous environments. Thickening and ageing of the oxide layer either in air-saturated solutions or during dry thermal exposures can reduce the anodic dissolution kinetics resulting in an increase in the E_{corr} (Sridhar et al., 1993b).

The measurements discussed earlier emphasize the need to monitor the E_{corr} in long-term laboratory and field immersion tests. Because the parameters used in calculating the E_{corr} from electrochemical models are uncertain, especially for highly irreversible reactions such as oxygen reduction, calibration of models from measured open-circuit potentials is necessary for using these in predicting the long-term evolution of corrosion potentials.

Several field experiences are reported to show the applicability of E_{rp} in predicting the occurrence of localized corrosion. Bernhardsson and Mellström (1983) reported failure due to pitting of alloy 825 compressor coolers on a gas lift platform. The environment was chlorinated seawater at 42 °C, and failure took place after 4 mo (minimum penetration rate was estimated to be about 5 mm/yr). The E_{rp}

for alloy 825 in 0.5 M chloride (the approximate concentration of chloride in seawater is 0.55 M) at 20 °C is 60 mV_{SCE} (Sridhar et al., 1995). Since the E_{rp} is expected to decrease with an increase in temperature and the E_{corr} in chlorinated seawater has been measured to be around 200 mV_{SCE} (Shaw et al., 1993), this in-service failure is consistent with the use of E_{rp} as a determining factor for the initiation of localized corrosion. In stagnant, aerated 3 percent NaCl solution at 60 °C, Bernhardsson and Mellström (1983) also found that type 316L SS underwent crevice corrosion after 2 mo while alloy 825 did not. Although these are still relatively short-term tests, the results are consistent with even shorter-term E_{rp} values. For example, Okayama et al. (1987) reported a value of −360 mV_{SCE} for E_{rp} of type 316 SS and −100 mV for alloy 825 in 3 percent NaCl at 80 °C. The E_{corr} of these alloys in aerated chloride solution at 95 °C has been reported (Sridhar et al., 1995) to be about −280 mV_{SCE} and is anticipated to increase slightly with a decrease in temperature due to higher solubility of oxygen. This value of E_{corr} is higher than the E_{rp} of type 316L SS and lower than that of alloy 825, thus explaining the localized corrosion of the former.

Protection against corrosion in highly oxidizing pulp and paper bleach plant washer fluids using controlled potential has been reported (Laliberte and Garner, 1981). In this case, the material is typically a type 317L SS (Fe-19Cr-12Ni-3.5Mo) and the E_{corr} in chlorine-containing waters is in the range of 100–500 mV_{SCE}, depending upon residual chlorine. This is far higher than the potential at which crevice corrosion was observed in potentiostatic tests (considered to be roughly equal to the E_{rp}). For type 317L SS in this environment (typically 1,000–5,000 ppm Cl^- and pH 2), the E_{rp} was measured to be about −30 mV_{SCE}. In these cases, cathodic protection by maintaining the potential at −500 mV_{SCE} has resulted in successful performance of the washer drums for over 10 yr.

In filtered natural seawater (mean temperature 25.2 °C), Kain (1993) observed crevice corrosion on type 316L SS after 60 days, but no crevice corrosion on alloy 59 (61Ni-22Cr-15Mo). Slight crevice corrosion was observed on alloy C-276 (Ni-16Cr-5Fe-16Mo-4W). Kain measured a E_{corr} in the range of 200–300 mV_{SCE}. In natural seawater, microbially enhanced cathodic reduction of oxygen is believed to be responsible for the high E_{corr} values. Again, the observed crevice corrosion of type 316L SS is consistent with the measured E_{rp} at this temperature of 0 mV_{SCE} (Okayama et al., 1987). A large number of Fe-Ni-Cr-Mo alloys was tested in natural, filtered seawater at 30 °C for 30 days by Hack (1982). The specimens were fitted with crevice washers of PTFE. In this limited duration test, alloys C-276 and 625 (Ni-22Cr-5Fe-9Mo-4Nb) suffered no localized corrosion, while type 316 SS and alloy 825 suffered significant crevice corrosion. The E_{rp} for alloy 825 in 0.5 M Cl^- is −60 mV_{SCE}, which is lower than the E_{corr} values reported for these alloys in natural seawater. An evaluation of all the published data on the E_{rp} values of alloy 825 and type 316/316L SS indicates that, if the chloride concentration becomes higher than approximately 0.5 M, alloy 825 may not be significantly better than type 316L SS in localized corrosion resistance.

4.4 MECHANISTIC CONSIDERATIONS OF INITIATION AND REPASSIVATION

Pit and crevice corrosion initiation have been thought of as originating from different processes. Pit initiation is well established as a stochastic process, with many metastable pits nucleating and repassivating dynamically on the metal surface below the critical potential for stable pit initiation. Crevice corrosion initiation has been traditionally thought of as a deterministic process dictated either by the development of a critical solution deep in the crevice such that the passive film is dissolved or a critical potential drop due to ohmic resistance of the crevice electrolyte such that active corrosion is initiated. However, recent evidence has shown that crevice corrosion in highly corrosion resistant alloys occurs essentially by the nucleation and growth of pits. Sridhar and Dunn (1994) showed that critical solution and potential drop did not occur until an increase in crevice current was detected, indicating that pits nucleated inside the crevice first (measured by an increase in current density) followed by growth of these pits to a sufficient spatial extent to affect crevice chemistry. Shinohara et al. (1993) used the Moire fringe technique to show that pits nucleated inside the crevice and then spread both in depth and lateral extent. Hence, at least for the corrosion resistant materials, a view of crevice corrosion is emerging (Laycock et al., 1996) where the crevice is thought to provide a long enough diffusion path to stabilize metastable pits. The observation of the similarity of E_{rp} for deep pits and crevices in this study reinforces this point of view.

The reader is referred to reviews on theories of pit initiation by Szklarska-Smialowska (1986) and Marcus and Oudar (1995). The theories can be classified as those that focus on the properties of the passive film and factors leading to the destabilization of the film and those that focus on processes in embryonic pits and factors leading to the stabilization of these pits. The present study indicates that the latter theories are more relevant to predicting the long-term initiation of localized corrosion. However, this does not imply that passive film properties are unimportant for the long-term initiation of localized corrosion of a material. Clearly, the passive film properties determine the evolution of corrosion potential which dictates the triggering of localized corrosion. Equally important, if the repassivation process is conceived as a competition between maintaining a concentrated chloride solution in nascent pits or the presence of a salt film and formation of a passive oxide film, then properties of passive films will play a role.

Burstein and Mattin (1996) proposed that the embryonic pits covered by the remains of the original oxide passive film acquire a critical solution chemistry due to metal dissolution inside them and consequent chloride ion migration. This solution may reach saturation with respect to metal chloride depending upon the dissolution rate (current) and volume of pit embryo. The presence of increased chloride concentration and lower pH due to hydrolysis results in a critical pit solution that maintains active dissolution of the metal inside the pit and an increase in the metastable pit size. From this point on, the metastable pit can adopt two paths: (i) the oxide film cover can rupture (perhaps due to osmotic pressures created by the chloride concentration difference between the inside and outside of the pit embryo) and the in-rushing external solution can dilute the pit solution and repassivate the pit, or (ii) the pit embryo can attain such a size that the oxide ruptures and in-rushing solution does not have a significant dilution effect so that the pit embryo continues to grow and becomes a stable pit. The path taken will be determined by many factors, including the dissolution current (applied potential), geometry, and external solution concentration. This concept is essentially similar to the pit initiation model originally proposed by Galvele (1976). If the applied potential is sufficiently high, continued dissolution of the metal helps to maintain the critical concentration and no repassivation occurs. If a crevice is present or the surface roughness is high, the transport path is lengthened and hence dilution by external solution is minimized,

also stabilizing the pit. Scully et al. (1996) also expressed this concept in terms of a critical ratio of pit current to pit radius (assuming hemispherical pits). The presence of a critical pit chemistry for repassivation has recently been experimentally verified by Sridhar and Dunn (1997).

If the above model is valid, the E_{rp} would be expected to continually decrease with depth of pit, since lengthening the transport path (radius of the pit) would mean less current (or potential) to maintain the critical pit chemistry. However, it should be noted that E_{rp} is an externally measured potential. The potential at the bottom of the pit (the pitting front) is decreased by ohmic resistance in the pit solution, which increases with pit depth. Hence, these competing factors would ensure that, in deep pits or crevices, the E_{rp} would become constant with pit depth. This is indeed observed in the present case.

The detrimental effect of $S_2O_3^{2-}$ on lowering E_{rp} can also be explained by the above mechanism. It has been shown that, in the active condition, $S_2O_3^{2-}$ adsorbs as atomic sulfur on the metal surface (Marcus and Oudar, 1995). Further, it has been shown that adsorbed sulfur increases the dissolution current from 5 to 12 times, depending upon the alloy system (Marcus and Oudar, 1995). In such a case, adsorbed sulfur will stabilize the pit embryo and prevent repassivation. Lower metal dissolution rates (lower applied potentials) would then be required to effect repassivation in the presence of $S_2O_3^{2-}$. The detrimental effect of reduced sulfur species may be important both because of the possibility of the presence of sulfate reducing bacteria near the HLW containers and the dissolution of sulfide inclusions in the metal.

5 CONCLUSIONS

The results of this investigation have shown that the repassivation potential for alloy 825 and type 316L SS is dependent on both the temperature and the composition of the environment. Numerous test techniques designed to test the adequacy of the repassivation potential have shown that pitting, crevice corrosion, and SSC cannot be initiated at potentials lower than the repassivation potential. In addition, after initiation, all localized corrosion ceases to propagate if the potential of the material is reduced below the repassivation potential. After repassivation, the corrosion rate of the material is determined by the passive current density.

Long-term testing of alloy 825 indicated that the corrosion potential under air-saturated conditions increased over a period of 600 days to values higher than E_{rp} measured in short-term experiments and crevice corrosion was observed when the corrosion potential was a few millivolts greater than the repassivation potential. Under these conditions, the propagation rate for localized corrosion will determine the lifetime of these materials. The long-term increase in corrosion potential is believed to be due to the growth and aging of the passive film. Similar increases in potential were observed on thermally aged film over shorter periods of time. Since many of the parameters in calculating the corrosion potential in an air-saturated environment are not known for the substrates of interest, the measured values of corrosion potential can be used to calibrate these calculations.

In order to judge the performance of a given alloy or container design over the expected performance period of a HLW container, it is necessary to characterize the environment contacting the container. Some of the key parameters include the time-dependent composition of the near field chemistry, especially chloride concentration, oxygen concentration, galvanic effects between various overpack materials, and temperature profiles of the WP. From the results of this investigation, it may be concluded that, for a given environment, the repassivation potential is conservative and an effective parameter to predict the long-term performance of corrosion resistant materials.

32/34

6 REFERENCES

American Society for Testing and Materials. 1996a. *Standard G-31-72, Standard Practice for Laboratory Immersion Corrosion Testing of Metals*. Vol. 3.02. Philadelphia, PA: American Society for Testing and Materials.

American Society for Testing and Materials. 1996b. *Standard G-5-94, Standard Reference Test Method for Making Potentiostatic and Potentiodynamic Anodic Polarization Measurements*. Vol. 3.02. Philadelphia, PA: American Society for Testing and Materials.

Bernhardsson, S., and R. Mellström. 1983. Performance of a highly alloyed stainless steel in marine environments. *CORROSION/83* Paper No. 72. Houston, TX: NACE International, Inc.

Burstein, G.T., and S.P. Mattin. 1996. The nucleation and early stages of growth of corrosion pits. *Critical Factors in Localized Corrosion II*. P.M. Natishan, R.G. Kelly, G.S. Frenkel, and R.C. Newman, eds. Volume 95-15. Pennington, NJ: The Electrochemical Society, Inc: 1–14.

Buscheck, T.A., J.J. Nitao, and L.D. Ramspott. 1996. Localized dryout: An approach for managing the thermal-hydrological effects of decay heat at Yucca Mountain. *Scientific Basis for Nuclear Waste Management XIX*. W.M. Murphy and D.A. Knecht, eds. Pittsburgh, PA: Materials Research Society: Symposium Proceedings 412: 715–722.

Cragnolino, G.A., and N. Sridhar. 1991. Localized corrosion of a candidate container material for high-level nuclear waste disposal. *Corrosion* 47(6): 464–472.

Cragnolino, G., D. Dunn, and N. Sridhar. 1996. Environmental factors in the stress corrosion cracking of type 316L stainless steel and alloy 825 in chloride solutions. *Corrosion* 52(3): 194–203.

Dunn, D.S., N. Sridhar, and G.A. Cragnolino. 1993. The effect of surface conditions on the localized corrosion of a candidate high-level nuclear waste container material. Corrosion control for Low cost reliability. *Proceedings of the Twelfth International Corrosion Congress*. Houston TX: NACE International: 4,021–4,030.

Dunn, D.S., N. Sridhar, and G.A. Cragnolino. 1995. Effects of surface chromium depletion on localized corrosion of alloy 825 as a high level nuclear waste container material. *Corrosion* 51(8): 618–624.

Dunn, D.S., N. Sridhar, and G.A. Cragnolino. 1996a. Long-term prediction of localized corrosion of alloy 825 in high-level nuclear waste repository environments. *Corrosion* 52(2): 115–124.

Dunn, D.S., G.A. Cragnolino, and N. Sridhar. 1996b. Localized corrosion initiation, propagation and repassivation of corrosion resistant high-level nuclear waste container materials. *CORROSION/96* Paper No. 97. Houston, TX: NACE International, Inc.

Frankel, G.S., J.R. Scully, and C.V. Jahnes. 1996. *Critical Factors in Localized Corrosion II*. P.M. Natishan, R.G. Kelly, G.S. Frenkel, and R.C. Newman, eds. Volume 95-15. Pennington, NJ: The Electrochemical Society, Inc: 30–40.

Galvele, J. 1976. Transport processes and the mechanism of pitting of metals. *Journal of Electrochemical Society* 123(4): 464–474.

Hack, H.P. 1982. Crevice corrosion behavior of 45 molybdenum-containing stainless steels in seawater. Paper No. 65. *Corrosion '82*. Houston TX: NACE International, Inc.

Kain, R.M. 1993. Seawater testing to assess the crevice corrosion resistance of stainless steels and related alloys. *Proceedings of the 12th International Corrosion Congress*. Houston, TX: NACE International, Inc: 1,889–1,900.

King, F., and M. Kolar. 1996. A numerical model for the corrosion of copper nuclear waste containers. *Scientific Basis for Nuclear Waste Management XIX*. W.M. Murphy and D.A. Knecht, eds. Pittsburgh, PA: Materials Research Society: Symposium Proceedings 412: 555–562.

Laliberte, L.H., and A. Garner. 1981. Corrosion protection of bleach plant washers by electrochemical potential control. *Tappi, The Journal of the Technical Association of Pulp and Paper Industry* 64(1): 47–51.

Laycock, N.J., M.H. Moayed, and R.C. Newman. 1996. Prediction of pitting potentials and critical pitting temperatures. *Critical Factors in Localized Corrosion II*. P.M. Natishan, R.G. Kelly, G.S. Frenkel, and R.C. Newman, eds. Volume 95-15. Pennington, NJ: The Electrochemical Society, Inc: 68–78.

Marcus, P., and J. Oudar, eds. 1995. *Corrosion Mechanisms in Theory and Practice*. New York, NY: Marcel Dekker, Inc.

Marsh, G.P., K.J. Taylor, I.D. Bland, C. Wescott, P.W. Tasker, and S.M. Sharland. 1986. Evaluation of the localized corrosion of carbon steel overpacks for nuclear waste disposal in granite environments. *Scientific Basis for Nuclear Waste Management IX*. L.W. Werme, ed. Pittsburgh, PA: Materials Research Society: Symposium Proceedings 50: 421–428.

Mohanty, S., G.A. Cragnolino, T. Ahn, D.S. Dunn, P.C. Lichtner, R.D. Manteufel, and N. Sridhar. 1996. *Engineered Barrier System Performance Assessment Code: EBSPAC Version 1.0β - Technical Description and User's Manual*. CNWRA 96-011. San Antonio, TX: Center for Nuclear Waste Regulatory Analyses.

Nakayama, T., and K. Sasa. 1976. Effect of ultrasonic waves on the pitting potentials of 18-8 stainless steel in sodium chloride solution. *Corrosion* 32: 283–285.

Nakayama, G., H. Wakamatsu, and M. Akashi. 1993. Critical conditions for the initiation of localized corrosion of mild steels in contact with bentonite used in geological disposal packages of nuclear waste. *Scientific Basis for Nuclear Waste Management XVI*. G.C. Interrante and R.T. Pabalan, eds. Pittsburgh, PA: Materials Research Society: Symposium Proceedings 294: 329–334.

Nakayama, G., H. Wakamatsu, and M. Akashi. 1993. Effects of chloride, bromide, and thiosulfate ions on the critical conditions for crevice corrosion of several stainless alloys as a material of geological disposal package for nuclear wastes. *Scientific Basis for Nuclear Waste Management XVI*. G.C. Interrante and R.T. Pabalan, eds. Pittsburgh, PA: Materials Research Society: 323–328.

Okayama, S., Y. Uesugi, and S. Tsujikawa. 1987. The effect of alloying elements on the repassivation potential for crevice corrosion of stainless steels in 3% NaCl solution. *Corrosion Engineering* 36: 157–168.

Pourbaix, M., L. Klimzack-Mathieu, C. Martens, J. Meunier, C. Vanlengenhaghe, L.D. Munch, J. Laureys, L. Nellmans, and M. Warzee. 1963. *Corrosion Science* 3: 239.

Rosenfeld, I.L., I.S. Danilov, and R.N. Oranskaya. 1978. Breakdown of the passive state and repassivation of stainless steels. *Journal of Electrochemical Society* 125(11): 1,729–1,735.

Roy, A.K., D.L. Fleming, and S.R. Gorton. 1996. Effect of chloride concentration and pH on pitting corrosion of waste package container materials. Paper 182. *Presented at the 190th Electrochemical Society Meeting*. Pennington, NJ: The Electrochemical Society, Inc.

Sagar, B. 1997. *NRC High Level Radioactive Waste Program Annual Progress Report—Fiscal Year 1996*. NUREG/CR-6513. No. 1: Washington, DC: Nuclear Regulatory Commission.

Scully, J.R., S.T. Pride, H.S. Scully, and J.L. Hudson. 1996. Some correlations between metastable pitting and pit stabilization in metals. *Critical Factors in Localized Corrosion II*. P.M. Natishan, R.G. Kelly, G.S. Frenkel, and R.C. Newman, eds. Volume 95-15. Pennington, NJ: The Electrochemical Society, Inc: 15–29.

Shaw, B.A., P.J. Moran, and P. Gartland. 1993. Crevice corrosion of a nickel-based superalloy in natural and chlorinated seawater. *Proceedings of the 12th International Corrosion Congress*. Houston, TX: NACE International, Inc: 1,915–1,928.

Shinohara, T., N. Masuko, and S. Tsujikawa. 1993. Moire method to measure penetration depth profiles on unevenly corroded metal surfaces. *Corrosion Science* 35: 785–789.

Shoesmith, D.W., F. King, and B.M. Ikeda. 1996. Indefinite containment of nuclear fuel wastes. *Scientific Basis for Nuclear Waste Management XIX*. W.M. Murphy and D.A. Knecht, eds. Pittsburgh, PA: Materials Research Society: Symposium Proceedings 412: 563–570.

Sridhar, N., and G.A. Cragnolino. 1993. Applicability of repassivation potential for long-term prediction of localized corrosion of alloy 825 and type 316L stainless steel. *Corrosion* 49(11): 885–894.

Sridhar, N., and D.S. Dunn. 1994. Effect of applied potential on changes in solution chemistry inside crevices on type 304L stainless steel and alloy 825. *Corrosion* 50: 857–872.

Sridhar, N., and D.S. Dunn. 1997. In-situ study of salt film stability in simulated pits of nickel by Raman spectroscopy. *The Journal of the Electrochemical Society*. Accepted for publication.

Sridhar, N., G.A. Cragnolino, and D.S. Dunn. 1993a. *Integrated Waste Package Experiments. NRC High-Level Radioactive Waste Research at CNWRA January—June 1993*. B Sagar, ed. CNWRA 93-01S. San Antonio, TX: Center for Nuclear Waste Regulatory Analyses.

Sridhar, N., G.A. Cragnolino, and D.S. Dunn. 1993b. *Experimental Investigations of Localized Corrosion of High-Level Waste Containers Materials*. CNWRA 93-004. San Antonio, TX: Center for Nuclear Waste Regulatory Analyses.

Sridhar, N., G.A. Cragnolino, and D.S. Dunn 1995. *Experimental Investigations of Failure Processes of High-Level Nuclear Waste Container Materials.* CNWRA 95-010. San Antonio, TX: Center for Nuclear Waste Regulatory Analyses.

Staehle, R.W. 1994. Combining design and corrosion for predicting life. *Life Prediction of Corrodible Structures.* R.N. Parkins, ed. Houston, TX: NACE International, Inc: 138–291.

Sugimoto, K., and K. Asano. 1990. Analysis of localized corrosion on stainless steel by micro-complex pH-pCl electrode. *Advances in Localized Corrosion.* H. Isaacs, V. Bertocci, J. Kruger, and S. Smialowska, eds. Houston, TX: NACE International, Inc: 375–379.

Szklarska-Smialowska, Z. 1986. *Pitting Corrosion of Metals.* Houston, TX: NACE International, Inc.

Thompson, N.G., and B.C. Syrett. 1992. Relationship between conventional pitting and protection potentials and a new, unique pitting potential. *Corrosion* 48: 649–659.

TRW Environmental Safety Systems, Inc. 1995. *Total System Performance Assessment – 1995: An Evaluation of the Potential Yucca Mountain Repository.* B00000000-01717-2200-00136. Las Vegas, NV: TRW Environmental Safety Systems, Inc.

TRW Environmental Safety Systems, Inc. 1996. *Mined Geologic Disposal System Advanced Conceptual Report. Vol. III of IV. Engineered Barrier System/Waste Package.* B00000000-01717-5705-00027. Rev. 00. Las Vegas, NV: TRW Environmental Safety Systems, Inc.

Tsujikawa, S., and Y. Hisamatsu. 1984. Repassivation potential as a crevice corrosion characteristic for austenitic and ferritic stainless steels. *Improvement of Corrosion Resistance of Structural Materials in Aggressive Media.* Ya. M. Koloyrkin, ed. Moscow, Russia: Nauka Publishers.

Tsujikawa, S., and Y. Kojima. 1991. Repassivation method to predict long-term integrity of low-alloy titanium for nuclear waste package. *Scientific Basis for Nuclear Waste Management XIV.* T. Abrajano and L.H. Johnson, eds. Pittsburgh, PA: Materials Research Society: Symposium Proceedings 212: 261–268.

U.S. Department of Energy. 1996. *Highlights of the Department of Energy's Updated Waste Containment and Isolation Strategy for the Yucca Mountain Site.* DOE Concurrence Draft. Washington DC: U.S. Department of Energy.

Wilde, B.E. 1974. On pitting and protection potentials: Their use and possible misuses for predicting localized corrosion resistance of stainless alloys in halide media. R.W. Staele, B.F. Brown, J. Kruger, and A. Agrawal eds. *Localized Corrosion*: 342–352.

Yashiro, H., and K. Tanno. 1990. The effect of electrolyte composition on the pitting and repassivation behavior of AISI 304 stainless steel at high temperature. *Corrosion Science* 31: 485–490.